Fases complexas em sistemas com interações competitivas

Daniel Adrián Stariolo

Departamento de Física
Universidade Federal do Rio Grande do Sul
Porto Alegre, Brazil

Sistemas (quase)-bidimensionais com interações competitivas

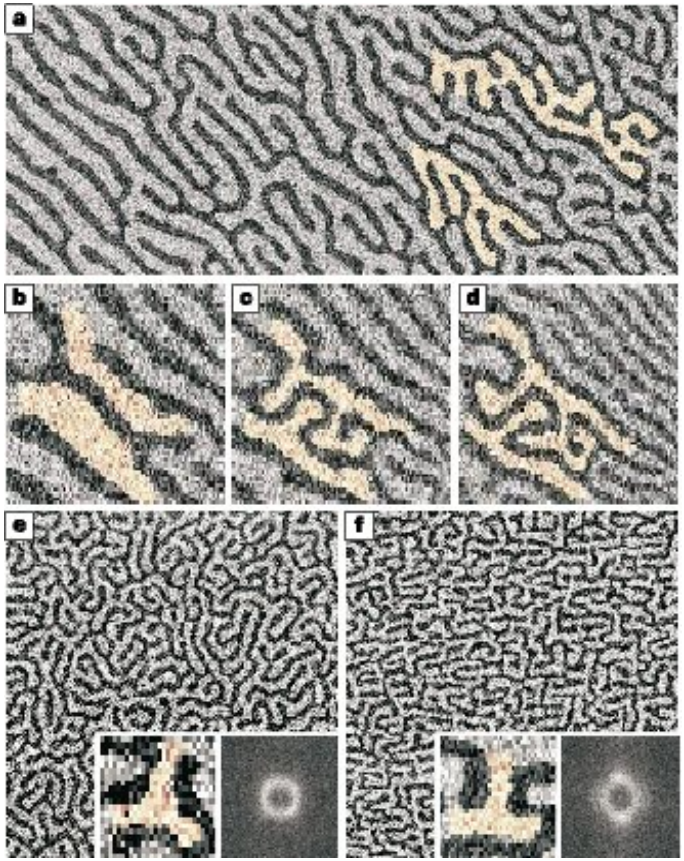

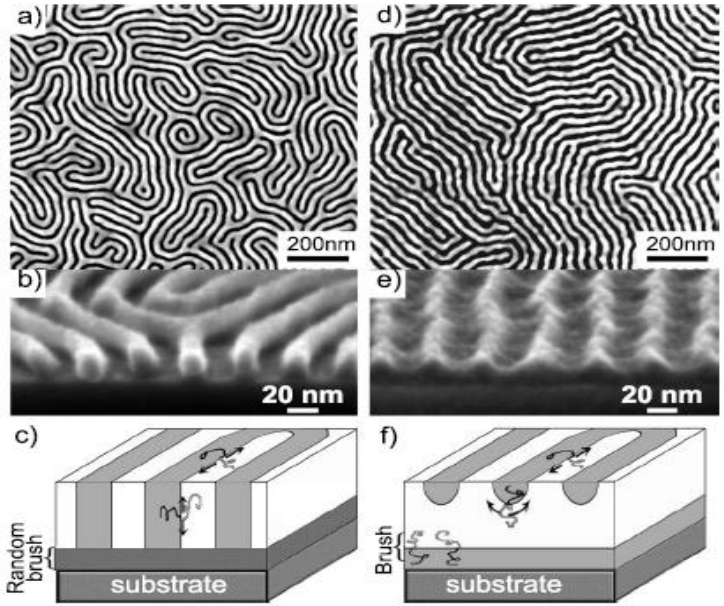

FIG. 1. Striped patterns from lamellar (left) and cylindrical (right) thin films: [(a) and (d)] top down scanning electron microscopy (SEM) of striped patterns, [(b) and (e)] cross section SEM after PMMA removal, and [(c) and (f)] cross section schematic of molecular arrangement showing possible directions for parallel diffusion (D_{par}).

Filmes ferromagnéticos ultrafinos de Fe/Cu(001)

O. Portmann *et al.* Nature **422**, 701 (2003)

Copolímeros de dibloco

R. Ruiz *et al.* Phys. Rev. B **77**, 054204 (2008)

Fluidos anisotrópicos

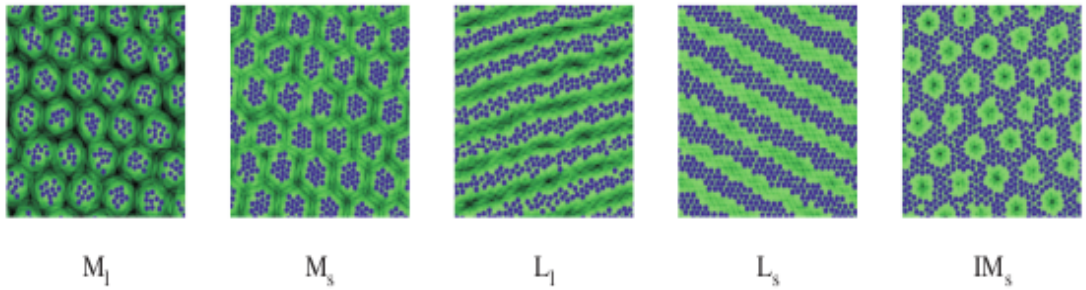

Fig. 1: (Color online) Snapshots from Monte Carlo simulations of the solid and liquid modulated phases of two-dimensional hard-core/soft-shoulder particles with $\sigma_s/\sigma = 5$; shown are the solid (M_s) and liquid (M_l) micelle phases, solid (L_s) and liquid (L_l) lamellar phases, and the solid inverse micelle phase (IM_s). The blue circles are the hard cores of the particles and the overlapping diffuse green circles represent their soft shoulders.

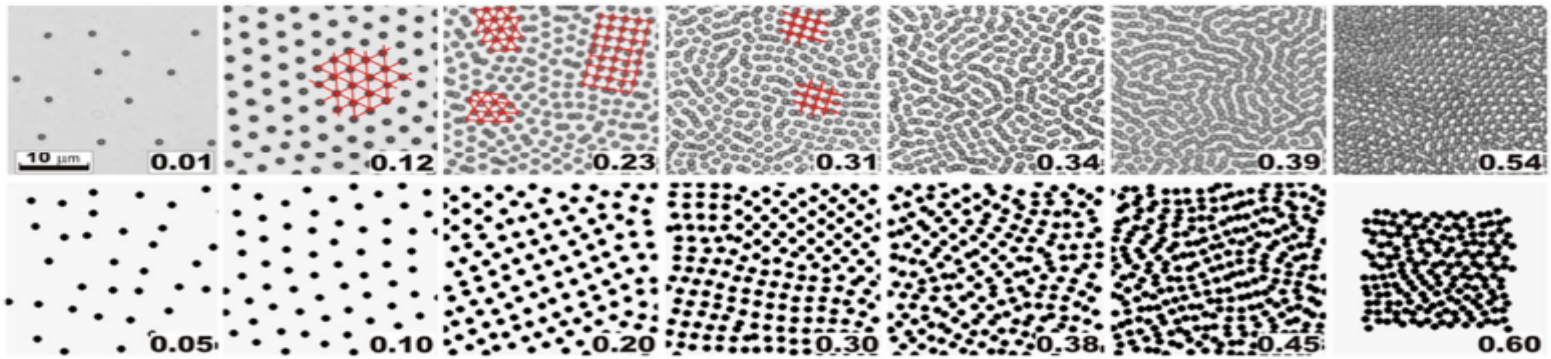

FIG. 2 (color online). Micrographs of the representative mesophases induced by varying the density (top row; $B = 12.5$ mT which gives $k \approx 400$) and the simulation snapshots (bottom row) labeled by the corresponding 2D volume fractions of colloids. Because of optical image distortion, the colloids on the micrographs appear slightly larger than their true size; in some of the micrographs, patches of the underlying lattices are emphasized to guide the eye. The reduced interaction strength of $k = 375$ was used in simulations at all but the largest two volume fractions where k was set to 125 to improve convergence; the number of particles $N = 1000$ except at $\eta = 0.60$, where $N = 200$.

Modelo de Ising frustrado com competição dipolar

$$\mathcal{H} = -\frac{J}{2} \sum_{<i,j>} S_i S_j + \frac{g}{2} \sum_{(i,j)} \frac{S_i S_j}{r_{ij}^3}$$

$$\mathcal{H} = -J \sum_{k_x,k_y} (\cos k_x + \cos k_y) |S_{\vec{k}}|^2 + \frac{g}{2} \sum_{k_x,k_y} (1 - bk) |S_{\vec{k}}|^2$$

No limite continuo

$$\mathcal{H} = \int \frac{d^2k}{(2\pi)^2} \phi(\vec{k}) \left[r_0 + (k - k_0)^2 + \ldots \right] \phi(-\vec{k}) + \ldots$$

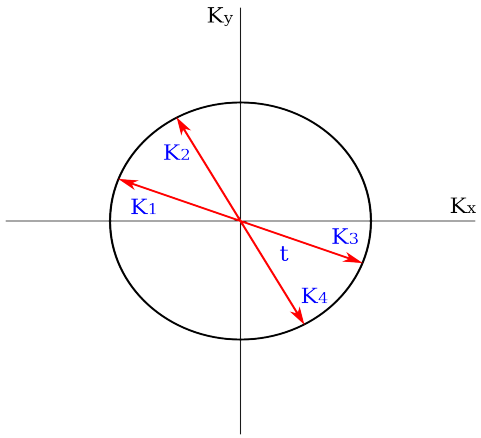

Modelo de Ising com competição dipolar

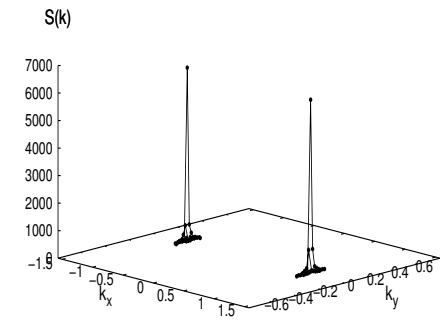

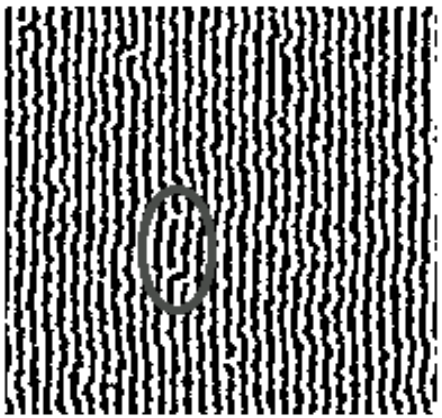

$\langle Q \rangle \sim 1$

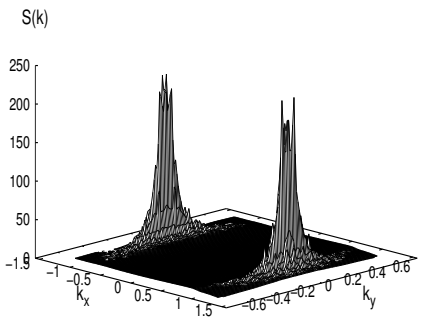

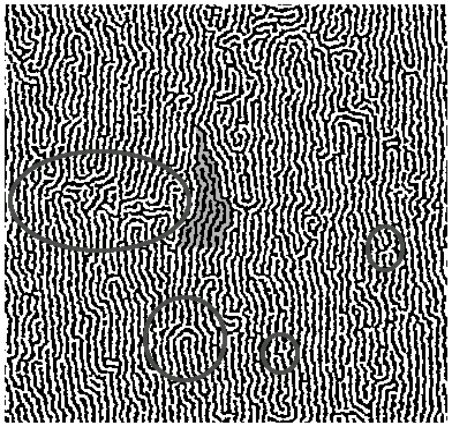

$\langle Q \rangle \sim 0.8$

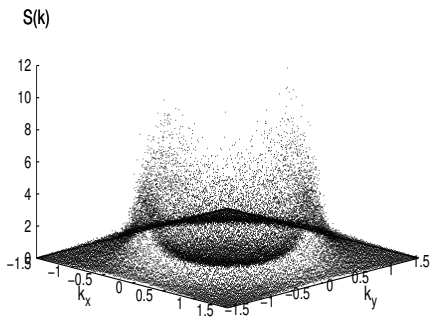

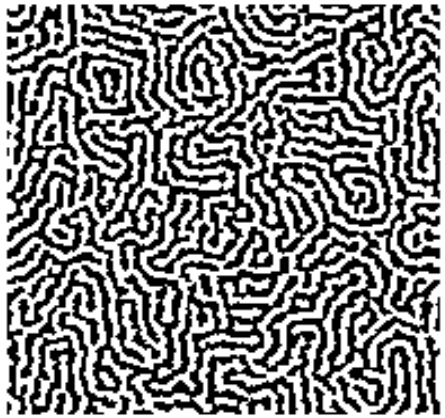

$\langle Q \rangle \sim 0.1$

L. Nicolao e D.A.S., PRB **76**, 054453 (2007)

Filme ferromagnético em campo externo

N. Saratz et al. PRL and PRB 2010

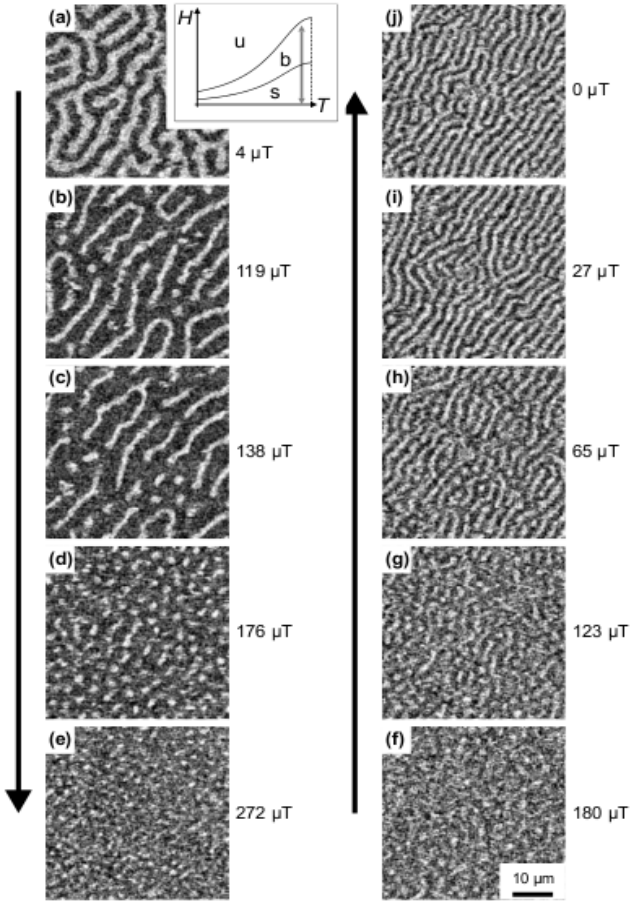

FIG. 2. Bubble formation upon changing the magnetic field at constant temperature. The absolute value of the magnetic field for each image is indicated. Images (a)–(e): increasing magnetic field at T/T_C=0.994 (T=350 K, d=2.00 ML), (f)–(j): decreasing magnetic field at T/T_C=0.996 (T=339 K, d=1.93 ML). All image sizes are 45 μm × 45 μm, the inset illustrates the path followed in the phase diagram.

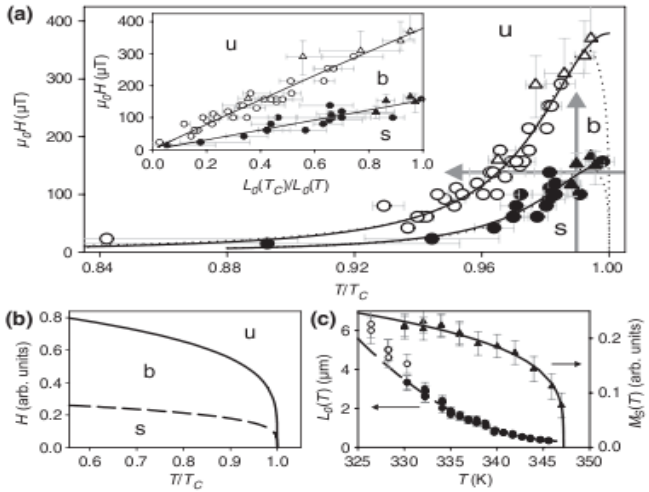

FIG. 2. Phase diagram and scaling of the transition fields. (a) Experimental phase diagram in $T - H$ space. The transition points obtained in constant field (circles) and at constant temperature (triangles) are shown for the transitions stripes ⟶ bubbles (solid symbols) and bubbles ⟶ uniform (open symbols). The gray arrows indicate the paths followed for the measurement of Fig. 1. The solid and dotted lines indicate fits to the transition lines using $1/L_0(T)$ and $M_S(T)/L_0(T)$ scaling, respectively, where $L_0(T)$ is the stripe width in zero field and $M_S(T)$ the local magnetization inside the domains [13]. The error bars indicate the upper and lower bounds for the transitions as determined from visual inspection of the SEMPA images. The scaled phase diagram (inset) demonstrates the $1/L_0(T)$ scaling of the transition fields. The solid lines are the same as in (a). (b) Standard phase diagram for modulated systems for comparison, adapted from Ref. [8]. (c) Experimental behavior of $M_S(T)$ (triangles, right scale) and $L_0(T)$ (circles, left scale). The lines are fits to the solid symbols using power laws $M_S(T) = M_\beta(1 - T/T_C)^\beta$ with $\beta \approx 0.25$ and $L_0(T) = L_0(T_C) + L_1(1 - T/T_C)^2$ [12]. The local magnetization $M_S(T)$ varies only weakly over most of the temperature range and rapidly drops to zero close to T_C. In contrast, $L_0(T)$ decreases strongly with increasing temperature, reaching a finite value $L_0(T_C)$ as T approaches T_C.

Filme ferromagnético em campo externo

Diagrama de fases de campo médio

$$\mathcal{H} = \frac{1}{2}\sum_{\vec{k}} \phi(\vec{k}) \left[r_0 + (k - k_0)^2 + \ldots \right] \phi(-\vec{k}) + u_0 \int d^2x \, \phi(\vec{x})^4$$

- $\phi_S(\vec{x}) = 2\sum_{n=0}^{\infty} m_n \cos(n\vec{k}_0 \cdot \vec{x})$
- $\phi_B(\vec{x}) = 2\sum_{n=0}^{\infty} m_n \sum_{i=1}^{3} \cos(n\vec{q}_i \cdot \vec{x})$
- S.A.Cannas, M.Carubelli, O.V.Billoni and D.A.S., PRB **84**, 014404 (2011)

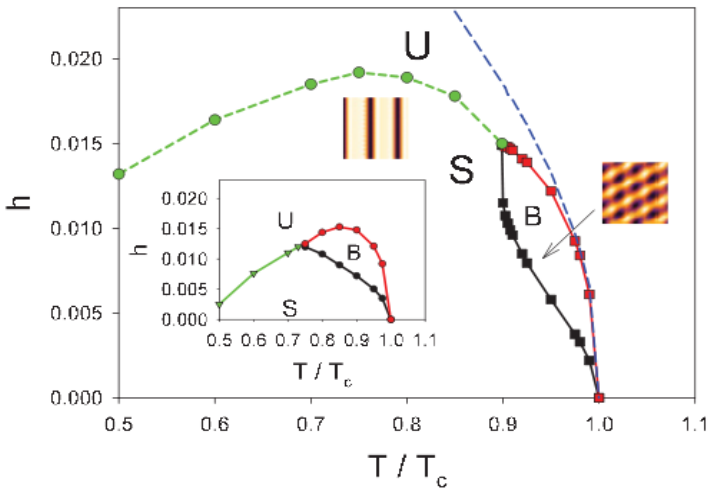

FIG. 3. (Color online) Phase diagram in the three-modes $n_{max} = 3$ approximation. Some typical configurations at the stripes and bubble phases are shown. The blue dashed line corresponds to the S spinodal line. The upper B spinodal line lies slightly below the S spinodal line, but both lines are indistinguishable at the present scales. The inset shows the phase diagram in the one-mode $n_{max} = 1$ approximation.

Filme ferromagnético em campo externo

Fases incomensuradas e perfis de modulação

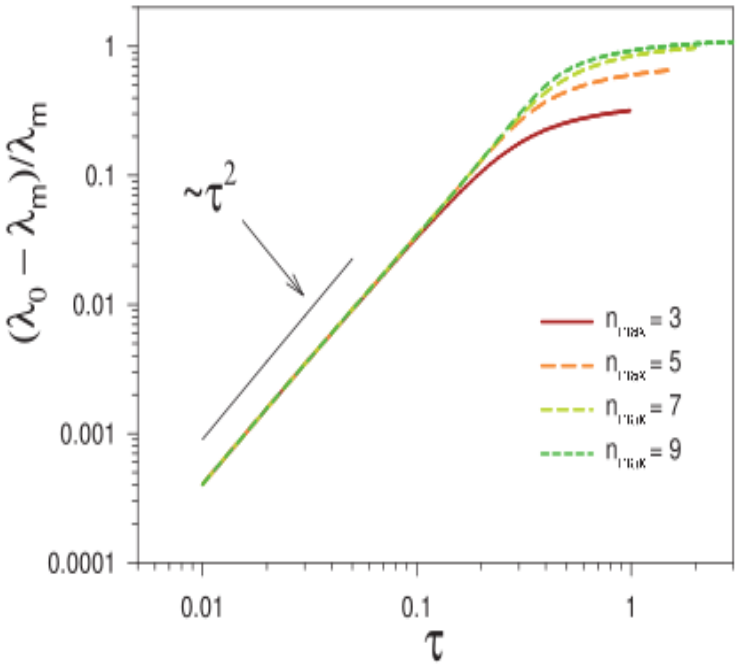

FIG. 1. (Color online) Stripe width variation with temperature at zero field for different values of $n_{\max}$.

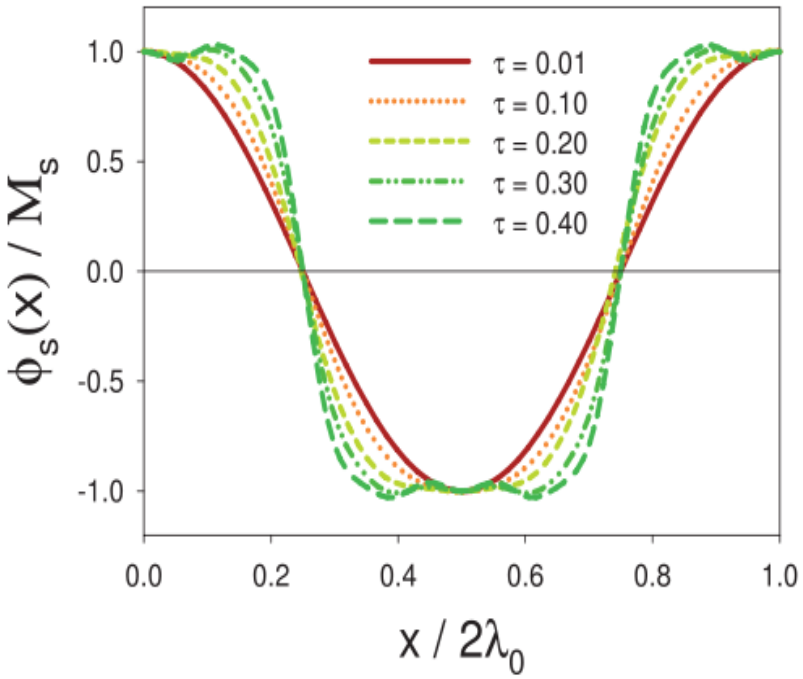

FIG. 2. (Color online) Change in the magnetization profile with temperature at zero field for $n_{\max} = 9$.

Flutuações: além do campo médio

Ordem nemática de interfases

$$\mathcal{H} = \frac{1}{2}\sum_{i,j}\left(J_{ij} - h_i K_{ij}\right) S_i S_j - \sum_i B_i S_i$$

Parâmetro de ordem nemático local

$$\langle Q_i \rangle = \frac{1}{\beta}\frac{\partial \ln Z}{\partial h_i} = \langle S_i S_{i+\hat{x}} - S_i S_{i+\hat{y}} \rangle$$

Parâmetro de ordem global

$$Q = \sum_i \langle Q_i \rangle = \sum_i \langle S_i S_{i+\hat{x}} - S_i S_{i+\hat{y}} \rangle = \frac{1}{2}\sum_{ij} K_{ij} \langle S_i S_j \rangle$$

O parâmetro de ordem é uma *média anisotrópica* da função de correlação de vizinhos próximos

O ferromagneto de Ising com frustração dipolar

$$\mathcal{H} = -J \sum_{<i,j>} S_i S_j + \sum_{(i,j)} \frac{S_i S_j}{r_{ij}^3}$$

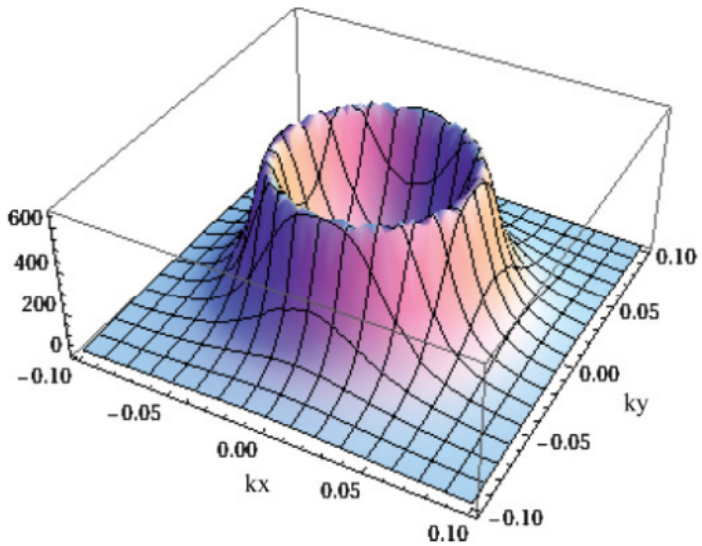

Fator de estrutura na fase isotrópica

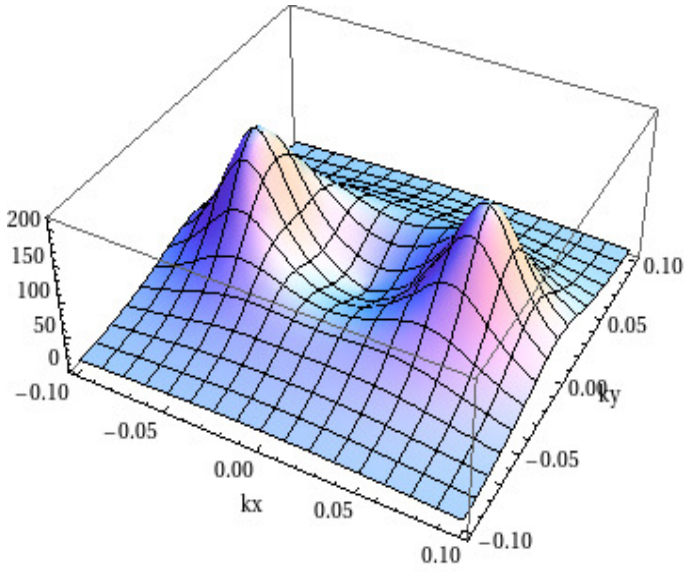

Fator de estrutura próximo da transição nemática-stripes

D.A.Barci and D.A.S., PRB **84**, 094439 (2011)

Possíveis linhas de trabalho futuro

- Em quais sistemas a fase nemática está presente ? Longo alcance versus alcance finito.
- Caracterização experimental das fases orientacionais (nemáticas) de interfases, em fluidos e sólidos.
- Simulação numérica de sistemas com interações de longo alcance.
- Modelagem da física em escala mesoscópica, identificação de parâmetros de ordem, renormalização.
- Simulação de fenômenos em escalas mesoscópicas.
- Dinâmica fora do equilíbrio, formação de padrões, dinâmica de defeitos, dinâmica lenta.

Colaboradores:

Daniel G Barci (Rio de Janeiro)
Orlando V Billoni (Córdoba)
Marianela Carubelli (Córdoba)
Sergio A Cannas (Córdoba)
Lucas Nicolao (Roma)
Alejandro Mendoza-Coto (Porto Alegre)
Luciana Velasque (Porto Alegre)
Alejandra Guerrero (Porto Alegre)
Deancarlo Degregori (Porto Alegre)